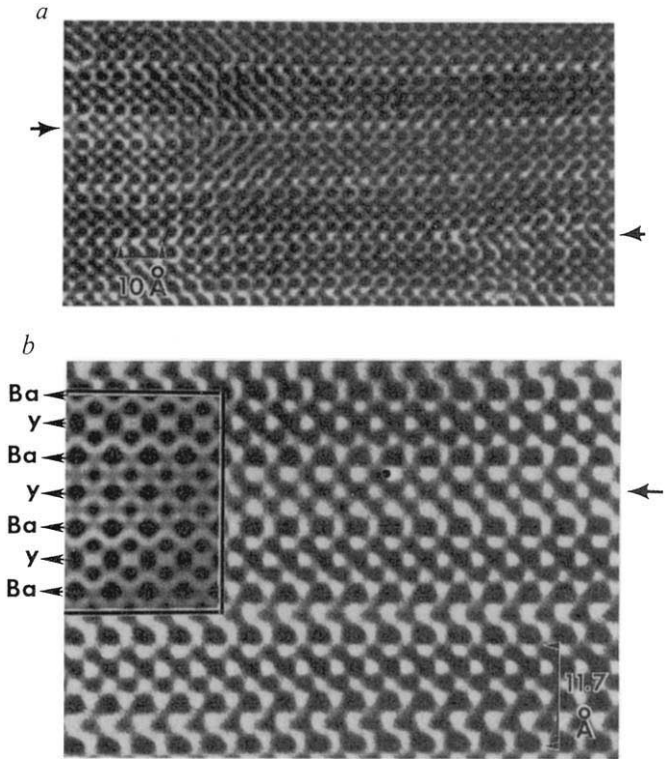

Fig. 4 *a*, Atomic structure image showing two planar faults (arrowed). *b*, High-magnification atomic structure image of region containing a planar fault (arrowed). Inset is the simulated image. Metal atom-columns are black. Sample thickness, 12 Å; defocus, −420 Å.

used the Pendellösung oscillations and image simulation to calibrate the sample thickness. Assuming that the metal atom positions and stoichiometry do not change systematically with thickness, our analysis of the thickness dependence of experimental images suggests that half of the oxygen sites in the basal Cu plane at $z = 0$ are empty. The resulting O-Cu-O chains lie perpendicular to plane of Fig. 2, and display long-range order over our field of view (~500 Å).

The planar defects in this material are of two types: twin boundaries and extrinsic planar faults. The twins come about as a consequence of the tetragonal to orthorhombic distortion and the accompanying formation of ordered oxygen chains in the basal planes. Thus, a twin boundary causes a 90° rotation in the direction of the O-Cu-O chains. The extrinsic planar faults are shown in Fig. 4. A search of naturally occurring (that is, low-energy) perovskite-related systems, including the K_2NiF_4 and barium titanate structures, suggests that these planar faults have the structure shown in Fig. 3*b*. They consist of a pair of planes similar to the basal planes at $z = 0$ separated by a Ba or Y layer; thus, the additional material has stoichiometry $ACuO_2$ (where A is Ba or Y). Comparison of experimental and simulated images suggests that Y is present at the midplane of the defect. This is consistent with Cu^{2+} at the fault planes, as shown in Fig. 3*b*. A system consisting of a periodic repetition of the entire structure shown in Fig. 3*b* has a stoichiometry of $Y_2Ba_2Cu_4O_9$, with an O/Cu ratio of 2.25. The stoichiometry of the perfect structure results in an O/Cu ratio of 2.33. As the experimentally measured O/Cu ratio is 2.30 (±0.02) (ref. 2), the above two values straddle the experimental measurement. We thus believe that these defects represent the material's response to stoichiometry constraints. However, unlike similar composition defects in other oxides (see, for example, ref. 12), all those we observe terminate within the crystal, indicating a slight misfit with the matrix. Note also that the presence of these defects results in a slight rotation of the planes on either side of the defect, which is evident from lattice images and their associated optical diffractograms, as well as from transmission electron diffraction patterns of this material. This may result from a 180° twinning of a slightly monoclinically distorted unit cell.

The presence of planar defects in $YBa_2Cu_3O_{6.9}$ must be taken into account in estimates of magnetic susceptibility, and may influence the electronic properties of the material through doping effects. The defects may also act as flux pinning sites, and thus be useful in optimizing extrinsic properties such as the critical current density and magnetic field. Finally, electrons may be localized on these planar faults, and some defects are known to provide strong electron-lattice coupling. But at present we have no means of determining whether defects play any direct role in the superconducting properties of these materials.

We acknowledge valuable discussions with Janet Brown, J. M. Cowley, W. J. Skocpol and S. Zahurak. The low-temperature experiments were partially supported by the NSF.

Note added in proof: We have recently learned of neutron diffraction experiments by J. J. Capponi *et al. Europhys. Lett.* **3**, 1301-1308 (1987) which also indicate the presence of long-range order in the oxygen vacancies.

Received 16 April; accepted 6 May 1987.

1. Bardeen, J., Cooper, L. N. & Schrieffer, J. R. *Phys. Rev.* **106**, 62 (1957).
2. Cava, R. J. *et al. Phys. Rev. Lett.* **58**, 1676-1679 (1987).
3. Siegrist, T., Sunshine, S., Murphy, D. W., Cava, R. J. & Zahurak, S. M. *Phys. Rev. B* (in the press).
4. Angle, R. *et al. Eos* **68**, 161 (1987).
5. Mattheiss, L. F. & Hamann, D. R. *Solid St. Commun.* (submitted).
6. Yu, J., Freeman, A. J. & Xu, J. H. *Phys. Rev. Lett.* **58**, 1035-1037 (1987).
7. Spence, J. C. H. & Tafto, J. *J. Microsc.* **130**, 147-154 (1983).
8. Goodman, P. & Moodie, A. *Acta crystallogr.* A**30**, 280-290 (1974).
9. Beyers, R. *et al. Appl. Phys. Lett.* (submitted).
10. Chen, C. H., Werder, D. J., Kwo, J. R., Liou, S. H. & Hong, M. *Phys. Rev. B* (in the press).
11. Anstis, G. R., Lynch, D. F., Moodie, A. F. & O'Keefe, M. A. *Acta crystallogr.* A**29**, 138-147 (1973).
12. Nobel Symposium *Chem. Scripta* **14** (1978-79).

Structure and crystal chemistry of the high-T_c superconductor $YBa_2Cu_3O_{7-x}$

W. I. F. David*, W. T. A. Harrison*, J. M. F. Gunn*, O. Moze*¶, A. K. Soper*, P. Day†, J. D. Jorgensen‡, D. G. Hinks‡, M. A. Beno‡, L. Soderholm‡, D. W. Capone II‡, I. K. Schuller‡, C. U. Segre§, K. Zhang§ & J. D. Grace||

* Neutron Division, Rutherford Appleton Laboratory, Chilton, Didcot OX11 0QX, UK
† Inorganic Chemistry Laboratory, South Parks Road, Oxford OX1 3QR, UK
‡ Argonne National Laboratory, Argonne, Illinois 60439, USA
§ Illinois Institute of Technology, Chicago, Illinois 60616, USA
|| Western Michigan University, Kalamazoo, Michigan 49008, USA

Materials within the phase diagram Y_2O_3–BaO–CuO have recently generated great interest because of the observation of superconductivity with a critical temperature (T_c) of ≥90 K[1,2]; the current consensus is that $YBa_2Cu_3O_{7-x}$ ($x \approx 0.2$) is the superconducting phase (see, for example ref. 3). Hazen *et al.*[4] concluded, from a single-crystal X-ray diffraction experiment, that its structure is based on the corner-linked octahedral perovskite structure: the tetragonal unit cell (space group $P\bar{4}m2$) arises from a tripling of the *c*-axis resulting from the ordering of yttrium and barium cations and associated oxygen defects. Here we present high-resolution neutron powder diffraction data for this phase with $x = 0.15$ (7). Our results agree with ref. 4 with respect to cation positions, but the location of one set of oxygen defects is substantially different and necessitates the lowering of lattice symmetry

¶ Present address: Istituto MASPEC del CNR, Via Chiavari 18/A, Parma 43100, Italy.

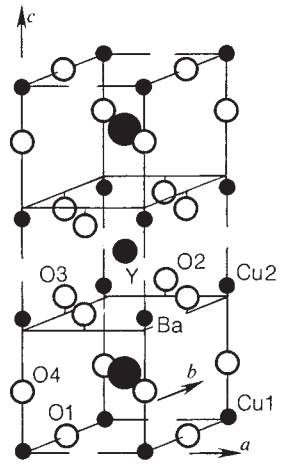

Fig. 1 The structure of $YBa_2Cu_3O_{6.85}$ showing the ordered stacking of yttrium, barium and oxygen defects along the *c*-axis. Cu(1) is square-planar coordinated; Cu(2) is surrounded by a square pyramid of oxygens.

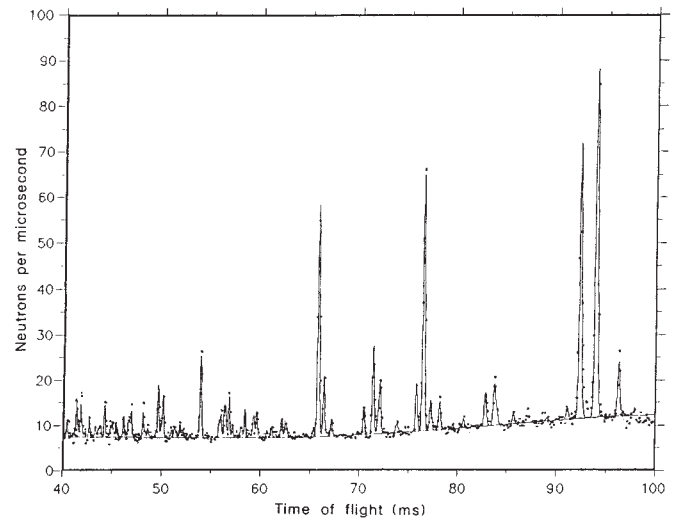

Fig. 2 Final observed (points) and calculated (line) profiles for $YBa_2Cu_3O_{6.85}$ time-of-flight powder neutron data. The *d*-spacings range from 0.8 to 2 Å in the figure. (A *d*-spacing of 1 Å corresponds to a time of flight of ~50 ms.)

from tetragonal to orthorhombic (space group *Pmmm*), in agreement with separate findings[5–8]. In contrast to the 35-K superconductor, $La_{1.85}Ba_{0.15}CuO_4$, the corner-linked CuO_4 planar groups are connected not only as sheets in the *a*–*b* plane but also as chains parallel to the *b*-axis. The average copper valence is 2.23 (5). From bond valence arguments we infer that the Cu^{2+} and Cu^{3+} ions preferentially occupy square pyramidal and square planar sites respectively. Crystal chemical considerations suggest that these structural features may be involved in the superconducting mechanism.

$YBa_2Cu_3O_{7-x}$ was prepared by high-temperature sintering of the appropriate oxides in an oxygen atmosphere. Powder neutron diffraction patterns were obtained at 80 K, 150 K and room temperature on the high-resolution powder diffractometer (HRPD) at the ISIS spallation neutron source, Rutherford Appleton Laboratory[9]. Results from only the room-temperature diffraction data are presented as no detectable change of structure was observed as a function of temperature. Simulation of the structure reported by Hazen *et al.*[4] showed clear structural similarities with the HRPD diffraction data. Lowering lattice symmetry by introducing a small orthorhombic distortion (space group symmetry reduction from $P\bar{4}m2$ to *Pmm*2) resulted in excellent agreement between observed and calculated peak positions. The space group symmetry was raised from *Pmm2* to *Pmmm* as no evidence for a lack of centre of symmetry was found.

Structural analysis was performed using the Rietveld method based on the Cambridge Crystallography Subroutine Library (CCSL)[10]. The cations were located before refinement in the positions obtained by Hazen *et al.*[4]. The positional parameters of all possible oxygen positions were based on the ideal perovskite structure and refined along with the oxygen site occupancies. Results of the profile refinement (Table 1) indicate two principal sets of oxygen vacancies compared with the ideal perovskite structure: one *a*–*b*-plane layer of oxygen ions surrounding the yttrium cation and one line of oxygen ions parallel to the *b*-axis (see Fig. 1). The location of the latter vacancies are significant, because, despite the pseudo-tetragonal lattice, no structural phase transition to tetragonal symmetry is possible in this material without the disordering of these oxygen vacancies. This is crucial to the understanding of superconductivity in these materials. Detailed analysis also showed that one site (O(2) at (1/2,0,0.3788(5))) was not fully occupied (92.5 ± 3.5% occupancy). A further site (O(1) at (0,1/2,0)) appeared to be slightly depleted and to possess an anomalously large thermal parameter: with the present quality of data the O(1) site occupancy and temperature factors were highly correlated and thus the O(1) site was constrained to be fully occupied. An anisotropic temperature factor was included in the refinement for O(1). No disordering of the yttrium and barium cations was detected. The refined chemical composition was calculated to be $YBa_2Cu_3O_{6.85(7)}$, corresponding to an average copper valence of 2.23(5) (23(5% Cu^{3+}: 77(5)% Cu^{2+}). The final χ^2 agreement factor $((R_{wP}/R_E))^2$ was 0.98 for 28 variable atomic and profile parameters and 302 reflections. Final observed and calculated profile plots are shown in Fig. 2.

Table 1 Final crystallographic data for $YBa_2Cu_3O_{6.85}$ at room temperature

Atom	Wyckoff symbol	*x*/*a*	*y*/*b*	*z*/*c*	*B** (Å²)	Site
Y	1h	1/2	1/2	1/2	0.9(1)	
Ba	2t	1/2	1/2	0.1844(5)	0.8(1)	
Cu(1)	1a	0	0	0	0.9(1)	
Cu(2)	2q	0	0	0.3554(3)	0.6(1)	
O(1)	1e	0	1/2	0	†	
O(2)	2s	1/2	0	0.3788(5)	0.3(4)	0.92(3)
O(3)	2r	0	1/2	0.3771(5)	0.6(1)	
O(4)	2q	0	0	0.1579(3)	0.8(1)	

Orthorhombic: space group *Pmmm* (no. 47); $a = 3.8187(2)$, $b = 3.8833(2)$, $c = 11.6687(6)$ Å.

* Isotropic temperature factor.

† For O(1), 3 anisotropic temperature factors were refined: $B_{11} = 4.8(6)$ Å², $B_{22} = 1.4(4)$ Å², $B_{33} = 2.5(6)$ Å²

$R_N = \sum |I_k(\text{obs}) - I_k(\text{calc})| / \sum I_k(\text{obs}) = 3.9\%$

$R_P = \sum |y_i(\text{obs}) - y_i(\text{calc})| / \sum y_i(\text{obs}) = 10.9\%$

$R_{wP} = \{\sum w_i[y_i(\text{obs}) - y_i(\text{calc})]^2 / \sum w_i y_i^2(\text{obs})\}^{1/2} = 11.7\%$

$R_E = \{[N - P + C] / \sum w_i y_i^2(\text{obs})\}^{1/2} = 11.8\%$

where *N*, *P* and *C* are the number of observations, parameters and constraints respectively.

The barium ions are tenfold coordinated by oxygen ions that form a cuboctahedron with two vertices missing. Yttrium is eightfold coordinated by an approximate cube of oxygen ions. Bond distances and angles for these polyhedra are typical of the species concerned. The copper ions sit in two crystallographically distinct and chemically dissimilar sites. One site (Cu(1) at (0,0,0)) is surrounded by a square planar oxygen configuration; the second site (Cu(2) at (0,0,0.3555(3))) is fivefold coordinated by a square pyramidal arrangement of oxygens. Table 2 lists selected bond lengths and angles for the room-temperature structure. The unexpectedly short Cu(1)–O(4) bond length of 1.843 Å, similar to that found in alkali metal cuprates such as $KCuO_2$ (ref. 11), prompted a bond strength calculation (Table 2) using the method of Brown and Wu[12]. This suggests that the Cu^{3+} ions preferentially occupy the square planar Cu(1) site at (0,0,0), a typical feature of d^8 ions. Indeed, locating Cu^{2+} and Cu^{3+} ions on square pyramidal, Cu(2), and square planar, Cu(1), sites respectively yields the stoichiometry $YBa_2Cu_3O_7$. Given

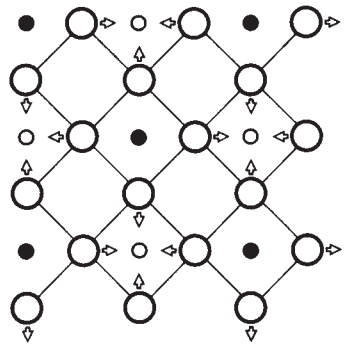

Fig. 3 Schematic view down the *z*-axis of the proposed in-plane breathing mode of the copper-oxygen sheets, leading to dynamic localization of electron pairs (Cu^{1+} character, closed circles) and electron vacancies (Cu^{3+} character, open circles). Large circles are oxygens.

the strong inference from bond strength calculations of an average valence of two on the square pyramidal site, the refined stoichiometry, $YBa_2Cu_3O_{6.85(7)}$, gives a 70(15)% : 30(15)% Cu^{3+} : Cu^{2+} distribution on the square planar site. These conclusions are at variance with a similar analysis by Capponi *et al.*[7], probably because of an incorrect choice of the unit strength distance parameter, D1, at 1.74 Å by these authors.

Although the structure of $YBa_2Cu_3O_{7-x}$ is substantially different from the 35-K superconductors $La_{1.85}A_{0.15}CuO_4$ (A = Ba, Sr), both structures may be considered to be derived from the perovskite structure and to contain corner-linked CuO_4 square planar arrangements. In $La_{1.85}A_{0.15}CuO_4$ these planar groups are two-dimensionally connected in the *a*–*b* plane and are derived from a Jahn–Teller-like elongated octahedral (4+2) coordination as in the parent La_2CuO_4 phase. In $YBa_2Cu_3O_{7-x}$ two types of planar groups exist: two thirds of the *a*–*b* planes containing copper consist of CuO_4 planar-like groups corner-linked in the *a*–*b* plane, derived from square pyramidal (4+1) coordination of the Cu(2) site at (0, 0, 0.3555(3)). These two-dimensional sheets are slightly puckered, with the copper displaced from the oxygen plane by ~0.262 Å towards the apical oxygen. The planar copper–oxygen bonds all lie between 1.93 and 1.96 Å. In addition, there are one-dimensional chains of true CuO_4 squashed planar groups oriented in the *b*–*c* plane and linked parallel to the *b*-axis; these are weakly bound to the *a*–*b*-plane CuO_4 planar groups by the long (2.308 Å) apical Cu–O bond of the square pyramid. There are no linkages between these square planar groupings in the *a* direction (see Fig. 1): this is reflected in the large anisotropic temperature factors for O(1).

It is likely that the sheets of corner-linked CuO_4 planar groups are involved in the superconducting mechanism because of their common occurrence in the $La_{2-x}Ba_xCuO_4$ and $YBa_2Cu_3O_{7-x}$ structures. An attractive chemical explanation for the occurrence of Cooper pairs in these sheets is the disproportionation of (d^9) Cu^{2+} into (d^{10}) Cu^+ and (d^8) Cu^{3+}, by analogy with the disproportionation of Au^+ and Au^{3+} in $Cs_2(Au^+Au^{3+})Cl_6$ (ref. 13). This leads to an electron configuration of $(d_{x^2-y^2})^0$ and $(d_{x^2-y^2})^2$ on alternate copper sites, which is equivalent to a dynamic localization of electron pairs. The dynamic emptying and filling of the $(d_{x^2-y^2})$ orbitals will isotropically contract and stretch the in-plane Cu–O bonds. The breathing mode associated with this effect, shown in Fig. 3, may be expected to behave anomalously around the superconducting transition temperature.

The observation of large temperature factors for O(1) suggests that the chains of CuO_4 planar groups parallel to the *b*-axis may also be associated with the superconducting mechanism. (These temperature factors may be reliably considered to be large, as examination of the variance–covariance matrix shows no substantial correlation between these and other variables. The temperature factors are similarly large when the O(1) site occupancy is also refined.) The large values of B_{11} and B_{33} indicate large low-frequency librational movements of the CuO_4 groups, but these modes are unlikely to be strongly coupled to the electron motion. The large value of B_{22}, indicative of a stretching and contraction of the Cu–O(1) bond, is more interesting as this mode has the correct symmetry to couple strongly the the electron motion in an analogous fashion to the breathing mode discussed above. Thus electron pairs may also be localized within these chains of CuO_4 planar groups. Another indication of the importance of these chains in the superconductivity is the fact that the bond lengths of the Cu–O bonds in the sheets and along the chains are respectively longer and shorter than in the lanthanum compounds. This implies that the copper electronic bands of the sheets should be more insulating in the yttrium case than the lanthanum case. Moreover the estimate of 30% Cu^{2+} along the chains implies no such tendency to insulating behaviour there. The existence of the chains in $YBa_2Cu_3O_{7-x}$ may therefore be the crucial structural feature in determining its high T_c.

Table 2 Selected bond distance, angle and strength data for $YBa_2Cu_3O_{6.85}$

Bond	Distance (Å)	Number	Bond	Distance (Å)	Number
Y–O(3)	2.387	×4	Cu(1)–O(4)	1.843	×2
Y–O(2)	2.402	×4	Cu(1)–O(1)	1.942	×2
Ba–O(4)	2.741	×4	Cu(2)–O(2)	1.929	×2
Ba–O(1)	2.877	×2	Cu(2)–O(3)	1.958	×2
Ba–O(3)	2.949	×2	Cu(2)–O(4)	2.306	×1
Ba–O(2)	2.986	×2			

Bond	Angle (deg)
O(1)–Cu(1)–O(1)	180
O(1)–Cu(1)–O(4)	90
O(2)–Cu(2)–O(3)	88.96
O(2)–Cu(2)–O(4)	98.14
O(3)–Cu(2)–O(4)	97.42

Bond strength data: Assuming:	Cu^{2+}	Cu^{3+}		
Cu(1)–O(4)	2×0.33	2×0.38		
Cu(1)–O(1)	2×0.24	2×0.26		
Summed strengths	2.27	2.56	≡ calculated valence	Cu(1)
Cu(2)–O(2)×2	2×0.23	2×0.25		
Cu(2)–O(3)×2	2×0.23	2×0.25		
Cu(2)–O(4)×1	0.17	0.16		
Summed strengths	2.01	2.16	≡ calculated valence	Cu(2)

Bond strengths, *s*, are calculated from bond lengths, *R*, using the formula, $s = (R_0/R)^N$, where R_0 is the bond length which corresponds to unit valence. For Cu^{2+} $R_0 = 1.718$, $N = 6.0$; for Cu^{3+} $R_0 = 1.771$, $N = 7.5$. Cu^{2+} values from Brown and Wu[10]; Cu^{3+} values derived from other Cu(III) salts by us. The average 'bond strength' valences of the copper sites may be used to provide an independent rough estimate of the chemical composition as $YBa_2Cu_3O_{6.64}$ (derived from Cu^{2+} parameters) and $YBa_2Cu_3O_{6.94}$ (derived from Cu^{3+} parameters): although reliance should not be placed on this formula, it is in broad agreement with the refined stoichiometry

We thank the Rutherford Appleton Laboratory for provision of neutron scattering facilities. Part of this work was supported by the US Department of Energy, BES-Materials Sciences.

Received 28 April; accepted 11 May 1987.

1. Wu, M. K. *et al. Phys. Rev. Lett.* **58**, 908–911 (1987).
2. Hinks, D. G. *et al. Appl. Phys. Lett.* (in the press).
3. Rao, C. N. R., Ganguly, P., Raychaudhuri, A. K., Mohan Ram, R. A. & Sreedhar, K. *Nature* **326**, 856–857 (1987).
4. Hazen, R. M. *et al. Phys. Rev. Lett.* (in the press).
5. Beno, M. A. *et al. Appl. Phys. Lett.* (in the press).
6. Greedan, J. E., O'Reilly, A. & Strager, C. V. *Phys. Rev.* (submitted).
7. Capponi, J. J. *et al. Europhys. Lett.* **3**, 301–308 (1987).
8. Beech, F., Miraglia, S., Santoro, A. & Roth, R. S. *Phys. Rev. Lett.* (submitted).
9. Johnson, M. W. & David, W. I. F. *Rutherford Appleton Lab. Rep.* No. 85/112 (1985).
10. Matthewman, J. C., Thompson, P. & Brown, P. J. *J. appl. Crystallogr.* **15**, 167–173 (1982).
11. Hestermann, K. & Hoppe, R. *Z. anorg. allg. Chem.* **367**, 249–253 (1969).
12. Brown, I. D. & Wu, K. K. *Acta crystallogr.* B**32**, 1957–1959 (1976).
13. Tindemans, J. C. M. & Verschoor, G. C. *Mater. Res. Bull.* **9**, 1947–1952 (1974).